Biometals (2010) 23:613–622
DOI 10.1007/s10534-010-9308-2

Electron paramagnetic studies of the copper and iron containing soluble ammonia monooxygenase from *Nitrosomonas europaea*

Stefan Gilch · Ortwin Meyer · Ingo Schmidt

Received: 16 July 2009 / Accepted: 12 February 2010 / Published online: 5 March 2010

Abstract Soluble ammonia monooxygenase (AMO) from *Nitrosomonas europaea* was purified to homogeneity and metals in the active sites of the enzyme (Cu, Fe) were analyzed by electron paramagnetic resonance (EPR) spectroscopy. EPR spectra were obtained for a type 2 Cu(II) site with $g_{\|} = 2.24$, $A_{\|} = 18.4$ mT and $g_{\perp} = 2.057$ as well as for heme and non heme iron present in purified soluble AMO from *N. europaea*. A second type 2 Cu(II) EPR signal with $g_{\|} = 2.29$, $A_{\|} = 16.1$ mT and $g_{\perp} = 2.03$ appeared in the spectrum of the ferricyanide oxidized enzyme and was attributed to oxidation of cuprous sites. Comparison of EPR-detectable Cu^{2+} with total copper determined by inductively coupled plasma-mass spectrometry (ICP-MS) suggests that there are six paramagnetic Cu^{2+} and three diamagnetic Cu^{1+} per heterotrimeric soluble AMO (two paramagnetic and one diamagnetic Cu per $\alpha\beta\gamma$-protomer). A trigonal EPR signal at $g = 6.01$, caused by a high-spin iron, indicative for cytochrome bound iron, and a rhombic signal at $g = 4.31$, characteristic of specifically bound Fe^{3+} was detectable. The binding of nitric oxide in the presence of reductant resulted in a ferrous $S = 3/2$ signal, characteristic of a ferrous nitrosyl complex. Inactivation of soluble AMO with acetylene did neither diminish the ferrous signal nor the intensity of the Cu^{2+}-EPR signal.

S. Gilch · O. Meyer · I. Schmidt (✉)
Lehrstuhl für Mikrobiologie, Universität Bayreuth, Bayreuth 95447, Germany
e-mail: ingo.schmidt1@uni-bayreuth.de

Keywords *Nitrosomonas europaea* · Soluble ammonia monooxygenase · Electron paramagnetic resonance · Copper and iron enzyme · Nitrogen oxide · Ferricyanide

Introduction

Nitrosomonas europaea is a chemolithoautotrophic bacterium which obtains all of its energy from the oxidation of ammonia (NH_3) to nitrite (NO_2^-) (Dua et al. 1979; Andersson and Hooper 1983; Hyman and Wood 1985; Prosser 1989; Schmidt and Bock 1997; Arp and Stein 2003). The carbon requirement for growth is covered by fixation of CO_2 via the Calvin–Benson–Bassham (CBB) cycle. Ammonia oxidation by *N. europaea* is mediated by two different enzymes, ammonia monooxygenase (AMO), which catalyzes the oxidation of NH_3 to hydroxylamine (NH_2OH) and hydroxylamine oxidoreductase (HAO), catalyzing the subsequent oxidation of NH_2OH to NO_2^- (Dua et al. 1979; Hollocher et al. 1981; Andersson and Hooper 1983). The second oxidation releases four electrons, two of which are required in ammonia oxidation and two of which are shuttled down the electron transport chain for cell growth and maintenance (Arp et al. 2002). *N. europaea* possesses a membrane bound AMO (McTavish et al. 1993; Hooper et al. 1997; Chain et al. 2003) and a soluble AMO (Schmidt and

Bock 1998; Gilch et al. 2009a). In vivo, both membrane-bound and soluble AMO oxidize ammonia and are therefore assumed to contribute to energy conservation (Gilch et al. 2009a). Soluble AMO has been purified as a heterotrimeric metalloenzyme consisting of the three subunits AmoA, AmoB, and cytochrome c_1 ($\alpha_3\beta_3\gamma_3$-subunit structure) with a molecular mass of about 317 kDa (Gilch et al. 2009a). Soluble AMO contains copper, iron and possibly zinc (Gilch et al. 2009a). Soluble AMO requires copper for activity and copper chelating agents (e.g., thiourea) inhibit ammonia oxidation activity (Loveless and Painter 1968; Ensign et al. 1993), so copper is proposed to participate in ammonia oxidation in an active site of the enzyme. Zahn and et al. (1996) suggested the presence of non-heme iron in AMO based on EPR studies of subcellular fractions, but a direct correlation between iron content and AMO activity could not be shown.

Acetylene is a mechanism-based inactivator of AMO (Andersson and Hooper 1983; Hyman and Wood 1985; Schmidt et al. 2001; Gilch et al. 2009b). Addition of [^{14}C]-acetylene to ammonia oxidizing *N. europaea* leads to an inhibition of ammonia oxidation activity (Hynes and Knowles 1978; Hyman and Wood 1985) due to a covalent attachment of acetylene to His 191 of AmoA (Gilch et al. 2009b). Acetylene also inhibits other monooxygenases like particulate methane monooxygenase (pMMO) from methanotrophic bacteria (Prior and Dalton 1985; Holmes et al. 1995; Balasubramanian and Rosenzweig 2007). Comparison of AMO and pMMO on genetic and functional level led to the assumption that location and co-ordination of the metal centers should be highly similar (McTavish et al. 1993; Holmes et al. 1995; Klotz and Norton 1998; Gilch et al. 2009a). Two metal centers, modeled as mononuclear and dinuclear copper sites, are located within the PmoB subunit. A third metal center, occupied by zinc, is located within the PmoC subunit (Lieberman and Rosenzweig 2005), but the site might contain copper in vivo (Balasubramanian and Rosenzweig 2007). The electron paramagnetic resonance spectrum of pMMO from *M. capsulatus* (Bath) indicates the presence of a type 2 Cu(II) center ($g_\perp = 2.057$, $g_\parallel = 2.24$, and $|A_\parallel| = 172$ G), a weak high-spin iron signal ($g = 6.01$), and a broad low-field ($g = 12.5$) signal, characteristic for reduced binuclear Fe(II)–Fe(II) centers. (Zahn and Dispirito 1996; Hendrich and Debrunner 1989; Lipscomb 1994). Treatment of reduced pMMO with nitric oxide produces a ferrous-nitric oxide derivative with an electron spin of $S = 3/2$ which is similar to those of other non-heme iron proteins with g values near 4 and 2 (Arciero et al. 1983; Arciero and Lipscomb 1986; Nelson 1987).

In this study, the function of copper and iron in soluble AMO was examined and the redox chemistry of the metal centers, the influence of nitric oxide, ferricyanide and the mechanism based inhibitor acetylene on the metal centers was analyzed.

Materials and methods

Growth of bacterium

Nitrosomonas europaea (ATCC 19718) was grown in a batch culture in mineral medium (Schmidt and Bock 1997) containing 50 mM NH_4Cl. Cultures were incubated at 28°C stirring at 50–200 rpm and aerated with 0.2–8 l air min^{-1} to maintain a oxygen concentration of 5 ± 0.2 mg l^{-1}. The pH was kept constant at 7.3 [20% (w/v) Na_2CO_3]. After 3 days, cells were harvested at $2 \times 10^8 \pm 3 \times 10^7$ cells ml^{-1}, concentrated by cross-flow filtration (Haemoflow HF80S, Fresenius Medical Care), and sedimented by centrifugation. The cell sediment was washed twice with mineral medium without ammonium. Purity of cultures was checked by plating on complex solid media or in liquid cultures as well as by phase-contrast microscopy.

Purification of soluble AMO

Cells were passed through a French pressure cell eight times with maximal pressure. The lysate was centrifuged at 8,000×*g* for 20 min at 4°C to remove unbroken cells. The supernatant was centrifuged at 120,000×*g* for 20 min at 4°C to prepare the soluble fraction. Soluble AMO was then purified 12-fold to homogeneity as described before (Gilch et al. 2009a) and transferred into a 50 mM K_2HPO_4/KH_2PO_4 buffer (pH 7.5, buffer A).

Production of acetylene and acetylene inactivated AMO

Acetylene was produced from barium carbide (BaC_2) according to Hyman and Arp (1990) and Gilch et al.

(2009a). In a closed glass bottle acetylene was produced from BaC_2 upon addition of water and was then dissolved in dimethyl sulphoxide (DMSO). To inactivate AMO, *N. europaea* cells (1 g) suspended in mineral medium without ammonium (4 ml) were transferred into a 25 ml-serum flask sealed with a butyl rubber stopper. NH_4Cl was added from a stock solution to a final concentration of 10 mM. After supplementing acetylene in DMSO bacteria were incubated at 28°C on a reciprocal shaker at 40 rpm. Inactivation of soluble AMO was considered complete when nitrite concentration remained constant. Soluble acetylene inactivated AMO was purified as described above.

Sample preparation for EPR spectroscopy

Potassium ferricyanide [$K_3Fe(CN)_6$] was added from a 100 mM stock solution to purified soluble AMO in buffer A to a final concentration of 2 mM. Samples were then subjected to gelfiltration on a Sephadex G-25-packed disposable column to remove unbound metals, transferred into quartz EPR tubes (Wilmad Lab Glass, Buena, USA) and frozen slowly in liquid N_2.

Reduced soluble AMO was produced by adding 1 mM ascorbate or 1 mM (10 mM) dithionite (DT) and 500 μM methoxyphenazine methosulfate (MPMS) as mediator. Reduction was performed in an anaerobic chamber under an oxygen-free N_2-atmosphere. Samples were reduced for 10 min and then frozen slowly in liquid nitrogen. To detect mixed-valency di-iron clusters purified soluble AMO was placed in an EPR tube, which was evacuated and flushed with oxygen-free N_2 several times to obtain anaerobic conditions. Ascorbate and MPMS were then added as anaerobic solutions and the sample was incubated 10 min prior to freezing and EPR measurements.

The nitric oxide derivatives of ascorbate and DT reduced soluble AMO were prepared by addition of nitric oxide to reduced soluble AMO under anaerobic conditions. Following formation of nitrosyl derivatives, the samples were transferred to quartz EPR tubes and frozen in liquid nitrogen as quickly as possible (<2 min).

Loosely bound bivalent metal ions were removed from soluble AMO by addition of Na_2-EDTA to a final concentration of 2 mM in buffer A. After incubation for 10 min the sample was subjected to gelfiltration onto a Sephadex G-25-packed disposable column equilibrated with buffer A, to remove Cu-EDTA and excess of Na_2-EDTA from the sample. An aliquot of soluble AMO was immediately transferred to quartz EPR tubes and frozen in liquid nitrogen. Remaining soluble AMO solution was supplemented with an appropriate $CuCl_2$ stock solution to a final concentration of 0.5 mM. To remove unbound Cu ions, the protein sample was loaded onto a Sephadex G-25-packed disposable column equilibrated with buffer A. Protein concentrations were determined before and after each gelfiltration to calculate the protein-metal ratio.

EPR measurements

All X-band EPR-spectra were recorded on an EMX spectrometer (Bruker, EPR spectrometer ECS 106) with a helium cryostat (Oxford instruments, ESR 900 cryostat) under experimental conditions described by Hänzelmann and Meyer (1998) and Bray et al. (1983). Samples (200 μl) were placed in a finger dewar filled with liquid nitrogen and quickly transferred to the precooled measuring chamber of the spectrometer. The concentration of Cu^{2+} in the sample was calculated by comparing the double spin integral with that of a 1 mM cupric perchlorate solution. The amount of non-heme iron was calculated by double spin integration of the high-spin Fe^{3+} signal at $g = 4.31$ (middle Kramers doublet; $3 \leftrightarrow 4$) as described by Bou-Abdallah and Chasteen (2008). As standard a 1 mM transferrin solution was applied. The range of integration was kept as narrow as possible (900 G) to avoid contribution of the underlying lower ($1 \leftrightarrow 2$) and upper ($5 \leftrightarrow 6$) Kramer doublets and to minimize the influence of the baseline and base line correction. The resonance signals at $g \sim 9.7$ and ~ 0.6 were not included in the integration because their intensity at microwave powers below 10 mW is too low (<1% with respect to the $g = 4.31$ signal) in comparison with the increasing uncertainty of a higher integration range (Aasa 1972; Bou-Abdallah and Chasteen 2008). Operating parameters of the EPR measurements are outlined in the respective figure legends.

Metal ion analysis and protein assay

Metal ions (Cu, Fe, Zn) in purified soluble AMO were determined by inductively coupled plasma-mass

spectrometry (ICP-MS). Samples (250 µl with 4.4 mg AMO ml^{-1}) were diluted in an equal volume of concentrated nitric acid and digested for 24 h at 110°C. Samples were diluted 40-fold with distilled water and the concentrations of metal ions were determined relative to standard solutions. Protein concentrations were determined by the biuret assay (Gornall et al. 1949).

Results

Prior to EPR measurements, the metal content of soluble AMO as well as of acetylene inhibited soluble AMO was determined by inductively coupled plasma-mass spectrometry. Isolated soluble AMO contains about 9.5 Cu, 3.9 Fe and 2.6 Zn atoms per molecule ($\alpha_3\beta_3\gamma_3$-subunit composition, Table 1). Soluble AMO with bound acetylene has a significantly reduced Cu content (7.1 Cu atoms per soluble AMO), but the Fe and Zn content is unchanged. The covalent binding of acetylene (ketene) to His 191 of AmoA (Gilch et al. 2009b), obviously removed about 2–3 Cu atoms from their co-ordination site(s) (Table 1).

Figure 1 shows the EPR spectrum of soluble AMO isolated from *N. europaea*. The EPR spectrum contains a high-spin Fe signal at $g = 6.01$, a symmetric rhombic ferric signal at $g = 4.31$ and a type 2 Cu(II) signal with $g_{\|} = 2.24$, $A_{\|} = 18.4$ mT and $g_{\perp} = 2.057$. A high-spin Fe(III) signal at $g = 6.01$ was already observed earlier analyzing membranes of *N. europaea* (Zahn et al. 1996). The type 2 Cu(II) signal indicates that metal ions in soluble AMO exist as active sites, electron or oxygen carriers. Furthermore, the type 2 Cu(II) signal is typical for a square planar or square pyramidal co-ordination of the Cu^{2+} ions. In pMMO of *M. capsulatus* (Bath) a similar type 2 Cu(II) signal with $g_{\perp} = 2.057$, $g_{\|} = 2.24$, and $|A_{\|}| = 172$ G was observed (Nguyen et al. 1994; Nguyen et al. 1996; Zahn and DiSpirito 1996).

Double spin integration of the type 2 Cu(II) signal and comparison to a cupric perchlorate standard indicated that 6.5 Cu^{2+} ions are bound to soluble AMO (317 kDa; $\alpha_3\beta_3\gamma_3$; Gilch et al. 2009a; Figs. 1, 2a). Taking into account, that ICP-MS analysis showed a total Cu content of 9.5 per soluble AMO (mol mol^{-1}, Table 1), soluble AMO contains three Cu^{1+} per native enzyme. Treatment of as-isolated soluble AMO with Na_2-EDTA reduced the Cu^{2+} content of the native enzyme from 6.5 to 3.1 (Fig. 2b). Thus 3.4 Cu^{2+} ions could be removed from soluble AMO by treatment with EDTA. Higher EDTA concentrations up to 50 mM were not able to detach further Cu^{2+} ions from their co-ordination sites within soluble AMO. This result shows that about three Cu^{2+} ions are resistant towards complexation by EDTA. It might be possible that these Cu^{2+} ions are not located close to the surface, but buried inside the enzyme shielding them from EDTA. Removal of EDTA and addition of $CuCl_2$ (0.5 mM) raised the Cu^{2+} content per soluble AMO to 4.1 (Fig. 2c). Hence, not all Cu^{2+} ions removed by EDTA can be reintroduced by the addition of $CuCl_2$. Application of $CuCl_2$ up to 10 mM had no significant effect on the Cu^{2+} occupancy of soluble AMO. Two different scenarios might explain this observation: First it could be assumed that Cu-integration into

Table 1 Metal content in the as-isolated soluble AMO and acetylene inhibited soluble AMO from *N. europaea*

Metal	AMO[a]			Acetylene labeled AMO[b]		
	Cu	Fe	Zn	Cu	Fe	Zn
Buffer (µM)	1.1 ± 0.3	0.4 ± 0.1	0.2 ± 0.1	0.6 ± 0.2	0.2 ± 0.1	0.2 ± 0.1
AMO in buffer (µM)	49.7 ± 4.7	20.7 ± 3.4	13.6 ± 2.3	27.8 ± 4.1	14.3 ± 2.5	10.8 ± 1.3
Metals per AMO (mol mol^{-1})[c]	9.5 ± 1.0	3.9 ± 0.7	2.6 ± 0.4	7.1 ± 1.0	3.7 ± 0.6	2.8 ± 0.3

Buffer Metal content of the protein free phosphate buffer (buffer A). *Soluble AMO in buffer* Metal content of soluble AMO and phosphate buffer (buffer A). Before metal analysis the soluble AMO samples were subjected to gel filtration. Data are average values of three replicated experiments (±SD)

[a] The AMO concentration was 1.63 mg ml^{-1}

[b] The AMO concentration was 1.21 mg ml^{-1}

[c] The metal content was calculated on the basis of a molecular mass of 317 kDa per AMO ($\alpha_3\beta_3\gamma_3$, Gilch et al. 2009a)

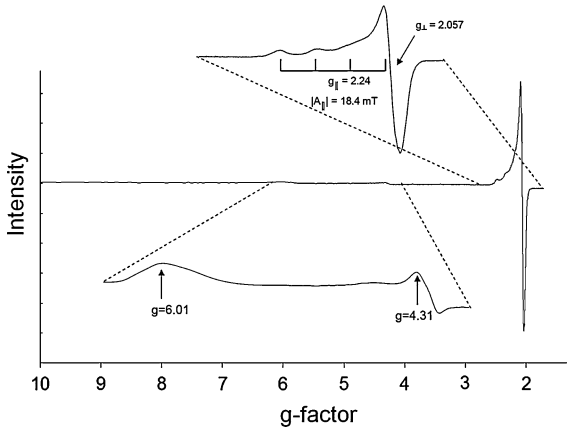

Fig. 1 X-band EPR spectrum of isolated soluble AMO from *N. europaea*. The protein concentration was 11.7 mg ml^{-1} in 50 mM K_2HPO_4/KH_2PO_4 buffer (pH 7.5). The spectrum was recorded at 10 K with 10 mW of microwave power, modulation amplitude of 10 G, modulation frequency of 100 kHz, and a time constant of 40 ms. The microwave frequency was 9.474 GHz

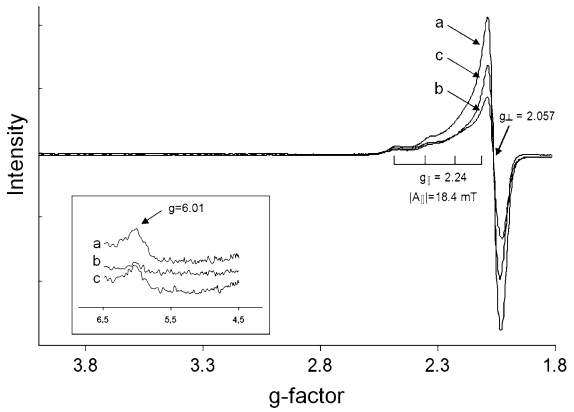

Fig. 2 X-band EPR spectra of as-isolated soluble AMO (*a*), soluble AMO after EDTA-treatment (*b*), and after subsequent addition of 0.5 mM $CuCl_2$ (*c*). The inlet shows the high spin iron signal at g = 6.01. Procedures for Cu removal with EDTA and Cu^{2+} supplementation with $CuCl_2$ are described in "Materials and methods" section. All spectra were recorded at 10 K with 10 mW of microwave power, modulation amplitude of 10 G, modulation frequency of 100 kHz, and a time constant of 40 ms. The microwave frequency was 9.474 GHz

soluble AMO must occur already before or during folding and assembling of the heterotrimeric protein complex. A second option is that Cu-integration requires the assistance of additional chaperons and/or Cu-chelatases, which are absent after purification of soluble AMO. EDTA treatment also affected the high spin iron signal at g = 6.01 (Fig. 2, inlet). Addition of EDTA nearly diminishes the iron signal (Fig. 2b), and incubation of iron-free AMO in 0.1 mM $FeSO_4$ solution reintroduced about 80% of the high-spin iron (Fig. 2c). On basis of the complex formation constants of the iron-EDTA (log $K_f = 14.32$) and the iron-cytochrome complex (log $K_f = 20.11$; Sanders et al. 1999) and the kinetics of the iron transfer at physiological conditions (25°C, pH 7), EDTA should not be able to remove iron from the cytochrome c_1-subunits of soluble AMO. The reason for the removal of heme-bound iron from cytochrome c_1 is still unknown, but the following hypotheses might explain this observation: First, iron in cytochrome c_1 might be bound by different ligands like it is known from other cytochromes and heme groups, respectively. The crystal structure of cytochrome c_1 from *N. europaea* is not resolved yet, and therefore a co-ordination of iron by weaker ligands in cytochrome c_1 can not be excluded. Second, the co-ordination of iron by cytochrome c_1 might be weaker than expected due to topological strain within this subunit. Conformational changes of cytochrome c_1 might be effected by its interaction with the other two subunits of soluble AMO (AmoA and AmoB). Third, changes in the redox state of cytochrome c_1 co-ordinated iron might influence the binding affinity towards the iron co-ordinating ligands. Oxidation of Fe(II) to Fe(III) significantly reduces the binding affinity towards heme (Sanders et al. 1999) and thus might allow metal removal by EDTA. It is assumed that cytochrome c_1 is involved in electron transfer to the active sites located in AmoA and AmoB (Gilch et al. 2009a) and hence cytochrome c_1 co-ordinated iron might be susceptible for redox chemistry.

From about nine Cu ions co-ordinated within soluble AMO about three are in the Cu^{1+}-state. Purification and EPR spectroscopy was performed under oxic conditions indicating that the three Cu^{1+} ions are resistant towards oxidation by molecular oxygen. Supplementing as-isolated soluble AMO with potassium ferricyanide $[K_3Fe(CN)_6]$ led to an almost complete oxidation of the Cu^{1+} ions (Fig. 3). Via double spin integration of the resulting type 2 Cu(II) signal a Cu^{2+} concentration of 8.8 Cu^{2+} per molecule of soluble AMO was calculated, which equals the number of Cu atoms determined by ICP-MS (Table 1). In addition to the type 2 Cu(II) signal

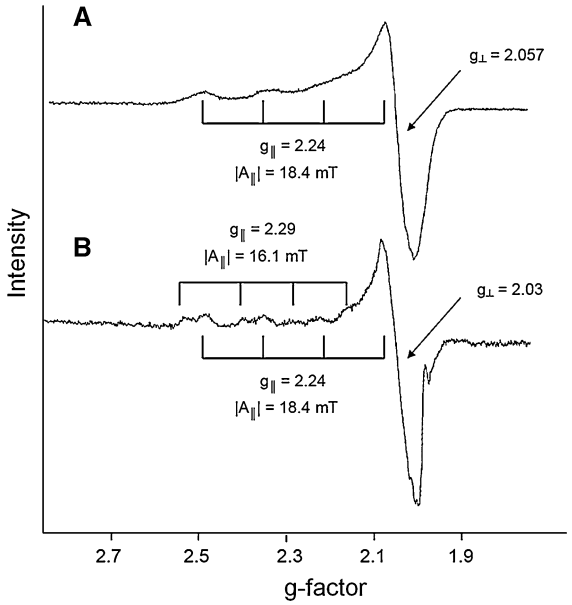

Fig. 3 X-band EPR spectra of as-isolated soluble AMO (*A*) and soluble AMO treated with 2 mM ferricyanide (*B*). Both spectra have been normalized for better comparison. Spectra were recorded at 10 K with 10 mW of microwave power, modulation amplitude of 10 G, modulation frequency of 100 kHz, and a time constant of 40 ms. The microwave frequency was 9.474 GHz

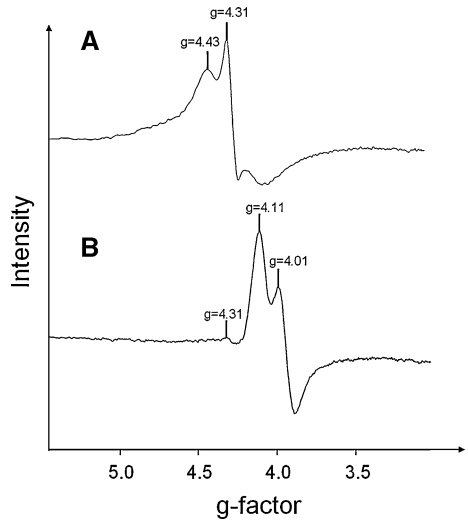

Fig. 4 X-band EPR spectra of DT-reduced soluble AMO (*A*) and DT-reduced soluble AMO treated with nitric oxide NO (*B*): both spectra have been normalized for better comparison. Spectra were recorded at 77 K with 2 mW of microwave power, modulation amplitude of 10 G, modulation frequency of 100 kHz, and a time constant of 40 ms. The microwave frequency was 9.474 GHz

($g_{\parallel} = 2.24$, $A_{\parallel} = 18.4$ mT and $g_{\perp} = 2.057$; Fig. 3A) the fully oxidized enzyme exhibits a second EPR signal with $g_{\parallel} = 2.29$, $A_{\parallel} = 16.1$ mT and $g_{\perp} = 2.03$ (Fig. 3B). Such signal is typically of Cu^{1+} sites oxidized by ferricyanide (Nguyen et al. 1998). Interestingly, the Cu^{1+} ions remain bound at the enzyme after being oxidized to Cu^{2+}. This fact provides evidence, that these Cu^{1+}-sites may function as redox active sites, involved in either electron transfer or substrate conversion. Structural Cu^{1+} atoms would be detached from the enzyme upon oxidation (Blain et al. 2002).

Nitric oxide (NO) has been commonly used to form EPR-active nitrosyl-iron complexes in some spectroscopically indistinguishable non-heme Fe^{3+} containing enzymes (Arciero et al. 1983; Nelson 1987; Zahn et al. 1996). Exposure of non-heme ferrous iron to NO can yield a species with an electron spin of S = 3/2. Based on this observation, EPR spectra of dithionite (DT)-reduced soluble AMO were recorded before and after treatment with NO. As it is obvious from Fig. 4B, a nitrosyl iron complex was formed resulting in a lower intensity of the rhombic signal at g = 4.31, and an intermediate spin (S = 3/2) appeared at g = 4.01 (isotropic nature) and g = 4.11 (rhombic nature). The rhombic signal at g = 4.43, typical for protein co-ordinated Fe^{3+}, vanishes completely after treatment with NO, indicating that all Fe^{3+} ions of soluble AMO were capable of forming a nitrosyl iron complex.

The EPR spectrum of the nitrosyl iron complex derivative of soluble AMO from *N. europaea* is similar to that of pMMO from *Methylosinus trichosporium* OB3b (Takeguchi and Okura 2000), *Methylococcus capsulatus* (Bath) (Zahn and DiSpirito 1996), and to protocatechuate-4,5-dioxygenase from *Pseudomonas testosteroni* (Lipscomb et al. 1982; Arciero and Lipscomb 1986). Protocatechuate-4,5-dioxygenase is thought to have a mononuclear non-heme iron in the active site, capable of reacting with NO and thus providing Fe-species with a spin state of S = 3/2 and g values around 4. However, it is still unclear whether Fe^{3+} plays a structural role on the tertiary folding of the protein or serves directly as electron transferring cluster or as an active site metal for substrate activation.

Purified soluble AMO contains about four iron atoms per molecule (Table 1). Three iron atoms are co-ordinated by the three Cyt c_1-subunits of native

soluble AMO in a high spin state, resulting in a trigonal signal at g = 6.01. Furthermore, the deviation from g = 6 is indicative for a weak rhombic distortion of the trigonal symmetry. To determine, whether the remaining iron atom might belong to a possible di-iron cluster [Fe(III)–Fe(III)], we attempted to evaluate conditions that would result in an EPR-visible mixed-valency form [Fe(III)–Fe(II)] of this type of cluster. Such a transition can be obtained after incubation of soluble AMO in the presence of the mediator MPMS and a reductant such as ascorbate or DT. This mixed-valency species normally has a strong S = 1/2 EPR signal, with all g-values below g = 6 (Andersson and Gräslund 1995). After reduction with ascorbate and MPMS such a signal was not observed, but the type 2 Cu(II) signal decreased, resulting from a partially reduction of EPR-active Cu^{2+} to EPR-silent Cu^{1+} (Fig. 5a). Interestingly, there was a significant increase in the rhombic high-spin (S = 5/2) Fe^{3+} signal at g = 4.31 with respect to oxidized soluble AMO (compare Figs. 1 and 5). This type of EPR signal originates from the middle Kramers doublet (3 ↔ 4) of high-spin Fe^{3+} with an |E/D| value of 0.33. Spin exchange coupling of high-spin Fe^{3+} with another paramagnetic metal can diminish the rhombic signal at g = 4.31. Upon reduction with ascorbate/MPMS the yet unidentified metal species (Z) was reduced, thus eliminating the magnetic spin exchange coupling with the rhombic Fe^{3+} ion, making it EPR-active (Fig. 5a). Several different possibilities exist for Z, such as: (i) a Cu^{2+} species; (ii) another Fe^{3+} species or (iii) a radical species such as tyrosyl or tyrosyl-derived radical as found in the copper enzymes galactose oxidase (Gerfen et al. 1996) or close to the Cu_{a3} in cytochrome *c* oxidase (MacMillan et al. 1999). The putative radical should then interact magnetically with the iron.

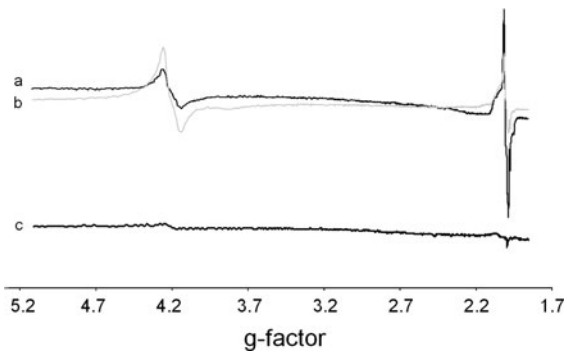

Fig. 5 X-band EPR-spectra of soluble AMO after reduction by ascorbate and DT. Soluble AMO was partially reduced with 1 mM ascorbate (*a*) and 1 mM DT (*b*) or fully reduced with 10 mM DT (*c*). Reduction was performed in the presence of the mediator MPMS (500 μM) and under anoxic conditions. Spectra were recorded at 10 K with 10 mW of microwave power, modulation amplitude of 10 G, modulation frequency of 100 kHz, and a time constant of 40 ms. The microwave frequency was 9.474 GHz

In relation to the spectrum of ascorbate/MPMS reduced soluble AMO, the spectrum of DT/MPMS reduced soluble AMO showed a further increased rhombic signal at g = 4.31 (Fig. 5b). The sharpness and the rhombic nature of this signal is characteristic of specifically bound Fe^{3+} ions in an octahedral ligation environment (Hagen 1992). The concentration of Fe^{3+} ions was estimated to be 0.85 Fe^{3+} per DT/MPMS reduced soluble AMO by integration of the rhombic Fe^{3+} signal against transferrin at two temperatures. Considering that three Fe are bound to the three mono-heme cytochrome c_1 subunits of soluble AMO, this result matches very well with the total amount of about 3.9 Fe atoms determined by ICP-MS (Table 1). The magnetic behavior of Fe^{3+} in soluble AMO is similar to that of transferrin, indicating a comparable ligation environment including co-ordination by tyrosine. A participation of tyrosine in Fe^{3+} co-ordination in AMO is further supported by the finding that Fe^{3+} is not reduced by ascorbate/MPMS or DT/MPMS which is a typical feature of iron-tyrosinate proteins (Que 1983; Que and Jo 1996).

The presence of non-heme iron agrees with the results of Zahn et al. (1996). Analyzing subcellular fractions of *N. europaea*, they detected non-heme Fe centers by EPR-spectroscopy, which they attributed to AMO. Evidence for a spin-coupled di-iron(III) center in the homologue enzyme pMMO was provided by Martinho et al. (2007) and Tumanova et al. (2008). They suggested that the dinuclear iron center is replaced by Zn in the crystal structure of pMMO and that this site is the active site of the enzyme, because such centers are the only type of centers known to oxidize methane to methanol at room temperature (Fox et al. 1988; Elango et al. 1997). In soluble AMO, Zn was also detectable (Table 1; Gilch et al. 2009a) and a replacement of non-heme Fe by Zn can not be excluded yet. Hence, in vivo soluble AMO might also contain dinuclear iron centers, which might have a catalytic function in the conversion of ammonia to hydroxylamine.

The exposure of soluble AMO to 1 mM DT and 1 mM ascorbate in the presence of the mediator MPMS resulted in a reduced type 2 Cu(II) signal (Fig. 5a, b). Complete reduction of all Cu^{2+} ions was observed upon addition of 10 mM DT under anaerobic conditions (Fig. 5c). The type 2 Cu(II) signal with $g_{||} = 2.24$ as well as the rhombic iron signal at $g = 4.31$ are diminished upon supplementation of excess of DT. Similar data have been reported for the type 2 Cu(II) signal of pMMO from *M. capsulatus* (Bath) (Nguyen et al. 1994; Nguyen et al. 1996).

Acetylene is a mechanism-based inhibitor of ammonia oxidation by soluble AMO and derivatizes the α-subunit (AmoA) of the enzyme (Hynes and Knowles 1978; Prior and Dalton 1985; Zahn et al. 1996; Yeager et al. 1999; Gilch et al. 2009b). The EPR spectra of soluble AMO with and without bound acetylene were recorded (Fig. 6). The lack of a significant effect of derivatization by acetylene on the type 2 Cu(II) signal suggests that acetylene does not bind at or nearby an active Cu^{2+} site of the enzyme. However, acetylene inhibited soluble AMO co-ordinates about 2.4 Cu atoms less than uninhibited soluble AMO (Table 1). Hence, acetylene might interact with or at an active site of the enzyme co-ordinating Cu^{1+} which is liberated upon acetylene binding. Considering that acetylene binds at His 191 of AmoA (Gilch et al. 2009b), the Cu^{1+} co-ordination site has to be located within the AmoA subunit of soluble AMO. Furthermore, acetylene inhibited soluble AMO exhibits a weak signal at $g = 2$, possibly originating from an organic radical, which might be formed upon binding of acetylene (Fig. 6).

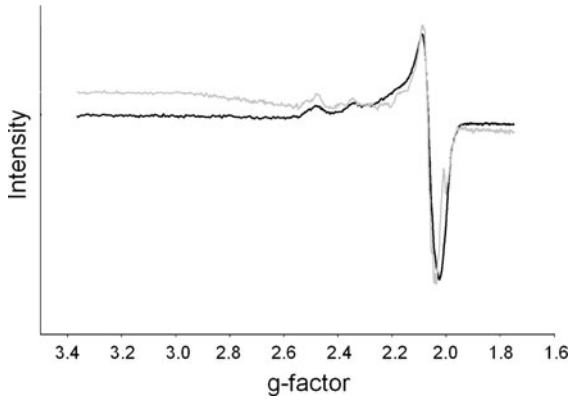

Fig. 6 X-band EPR spectra of air-oxidized uninhibited soluble AMO (*black line*) and acetylene inhibited soluble AMO (*grey line*). Spectra were recorded at 10 K with 10 mW of microwave power, modulation amplitude of 10 G, modulation frequency of 100 kHz, and a time constant of 40 ms. The microwave frequency was 9.474 GHz

It is unknown, if the Cu^{1+} containing site of AmoA resembles a monomeric, dimeric or even trimeric Cu center. The nuclearity of biological copper centers is not correlated with reactivity, leaving open the possibility that any of the copper sites could be the catalytic one. The observation, that binding of acetylene to His 191 of AmoA decreases only the Cu^{1+} and not the Cu^{2+} occupancy of soluble AMO leads to the assumption, that AmoA harbors a mononuclear Cu^{1+} site, possibly co-ordinated by the motif Asp 187-X_3-His 191-X_{12}-His 204 (Gilch et al. 2009a). This is due to the fact, that a loss of Cu^{1+} would destroy the integrity of a mixed-valency dinuclear Cu^{1+}–Cu^{2+} center resulting in a subsequent loss of the Cu^{2+}, which was not detectable in our experiments (Fig. 6). This assumption is further supported by the presence of two different type 2 Cu(II) signals after reduction of the Cu^{1+} site with potassium ferricyanide (Fig. 3B), indicating different co-ordination environments for the Cu^{1+} and the Cu^{2+} sites.

Acknowledgment This work was financially supported by the Deutsche Forschungsgemeinschaft (DFG). We thank Dr. Vitali Svetlitchnyi for helpful discussion and for excellent assistance performing the EPR experiments.

References

Aasa R (1972) Re-interpreatation of the electron paramagnetic resonance spectra of transferrins. Biochem Biophys Res Commun 49:806–812

Andersson KK, Gräslund A (1995) Diiron-oxygen proteins. In: Sykes AG (ed) Advances in inorganic chemistry, vol 43. Academic Press, Orlando, pp 308–359

Andersson KK, Hooper AB (1983) O_2 and H_2O are each the source of one O in NO_2^- produced from NH_3 by *Nitrosomonas*; ^{15}N-NMR evidence. FEBS Lett 164:236–240

Arciero DM, Lipscomb JD (1986) Binding of 17O-labeled substrate and inhibitors to protocatechuate 4,5-dioxygenase-nitrosyl complex. J Biol Chem 261:2170–2178

Arciero DM, Lipscomb JD, Huynh BH, Kent TA, Münck E (1983) Evidence for direct substrate binding to the active site Fe^{2+} of extradiol dioxygenases. J Biol Chem 258:14981–14991

Arp DJ, Stein LY (2003) Metabolism of inorganic N compounds by ammonia-oxidizing bacteria. Crit Rev Biochem Mol Bio 38:471–495

Arp DJ, Sayavedra-Soto LA, Hommes NG (2002) Molecular biology and biochemistry of ammonia oxidation by *Nitrosomonas europaea*. Arch Microbiol 178:250–255

Balasubramanian R, Rosenzweig AC (2007) Structural and mechanistic insights into methane oxidation by particulate methane monooxygenase. Acc Chem Res 40:573–580

Blain I, Slama P, Giorgi M, Tron T, Réglier M (2002) Copper containing monooxygenases: enzymatic and biomimetic studies of the O-atom transfer catalysis. Rev Mol Biotech 90:95–112

Bou-Abdallah F, Chasteen ND (2008) Spin concentration measurements of high-spin ($g' = 4.3$) rhombic iron(III) ions in biological samples: theory and application. J Biol Inorg Chem 13:15–24

Bray RC, George GN, Lange R, Meyer O (1983) Studies by e.p.r. spectroscopy of carbon monoxide oxidases from *Pseudomonas carboxydovorans* and *Pseudomonas carboxydohydrogena*. Biochem J 211:687–694

Chain PP, Lamerdin J, Larimer F, Regala W, Lao V, Land M, Hauser L, Hooper AB, Klotz MG et al (2003) Complete genome sequence of the ammonia-oxidizing bacterium and obligate chemolithoautotroph *Nitrosomonas europaea*. J Bacteriol 185:2759–2773

Dua RD, Bhandari B, Nicholas DJD (1979) Stable isotope studies on the oxidation of ammonia to hydroxylamine by *Nitrosomonas europaea*. FEBS Lett 106:401–404

Elango N, Radhakrishnan R, Froland WA, Wallar BJ, Earhart CA, Lipscomb JD, Ohlendorf DH (1997) Crystal structure of the hydroxylase component of methane monooxygenase from *Methylosinus trichosporium* OB3b. Protein Sci 6:556–568

Ensign SA, Hyman MR, Arp DJ (1993) In vitro activation of ammonia monooxygenase from *Nitrosomonas europaea* by copper. J Bacteriol 175:1971–1980

Fox BG, Surerus KK, Münck E, Lipscomb JD (1988) Evidence for a mu-oxo-bridged binuclear iron cluster in the hydroxylase component of methane monooxygenase. Mössbauer and EPR studies. J Biol Chem 263:10553–10556

Gerfen GJ, Bellew BF, Griffin RG, Singel DJ, Ekberg CA, Whittaker JW (1996) High-frequency electron paramagnetic resonance spectroscopy of the apogalactose oxidase radical. J Phys Chem 100:16739–16748

Gilch S, Meyer O, Schmidt I (2009a) A soluble form of ammonia monooxygenase from *Nitrosomonas europaea*. Biol Chem 390:863–873

Gilch S, Vogel M, Lorenz MW, Meyer O, Schmidt I (2009b) Interaction of the mechanism-based inactivator acetylene with ammonia monooxygenase of *Nitrosomonas europaea*. Microbiology 115:279–284

Gornall AG, Bardawill CJ, David MM (1949) Determination of serum proteins by means of the biuret reaction. J Biol Chem 177:751–766

Hagen WR (1992) EPR spectroscopy of iron-sulfur proteins. In: Sykes AG (ed) Advances in inorganic chemistry, vol 38. Academic Press, Orlando, pp 359–408

Hänzelmann P, Meyer O (1998) Effect of molybdate and tungstate on the biosynthesis of CO dehydrogenase and the molybdopterin cytosine-dinucleotide-type of molybdenum cofactor in *Hydrogenophaga pseudoflava*. Eur J Biochem 255:755–765

Hendrich WP, Debrunner PG (1989) Integer-spin electron paramagnetic resonance of iron proteins. Biophys J 56:489–506

Hollocher TC, Kumar S, Nicholas DJD (1981) Oxidation of ammonia by *Nitrosomonas europaea*: definitive ^{18}O-tracer evidence that hydroxylamine formation involves a monooxygenase. J Biol Chem 256:10834–10836

Holmes AJ, Costello A, Lidstrom ME, Murrell JC (1995) Evidence that particulate methane monooxygenase and ammonia monooxygenase may be evolutionarily related. FEMS Microbiol Lett 132:203–208

Hooper AB, Vannelli T, Bergmann DJ, Arciero DM (1997) Enzymology of the oxidation of ammonia to nitrite by bacteria. Antonie van Leeuwenhoek 71:59–67

Hyman MR, Arp DJ (1990) The small-scale production of [U-^{14}C]acetylene from $Ba^{14}CO_3$: application to labeling of ammonia monooxygenase in autotrophic nitrifying bacteria. Anal Biochem 190:348–353

Hyman MR, Wood PM (1985) Suicidal inactivation and labelling of ammonia monooxygenase by acetylene. Biochem J 227:719–725

Hynes RK, Knowles R (1978) Inhibition by acetylene of ammonia oxidation *in Nitrosomonas europaea*. FEMS Microbiol Lett 4:319–321

Klotz MG, Norton JM (1998) Multiple copies of ammonia monooxygenase (amo) operons have evolved under biased AT/GC mutational pressure in ammonia-oxidizing autotrophic bacteria. FEMS Microbiol Lett 168:303–311

Lieberman RL, Rosenzweig AC (2005) Crystal structure of a membrane-bound metalloenzyme that catalyses the biological oxidation of methane. Nature 434:177–182

Lipscomb JD (1994) Biochemistry of the soluble methane monooxygenase. Annu Rev Biochem 48:371–399

Lipscomb JD, Whittaker JW, Arciero DM (1982) Comparative studies of intra- and extradiol protocatechuate dioxyphases. In: Nizaju S, Yamamoto Y, Ishimura M, Coon L, Ernster L, Estabrook RW (eds) Oxygenases and oxygen metabolism. Academic Press, New York, pp 27–38

Loveless JE, Painter HA (1968) The influence of metal ion concentrations and pH value on the growth of a *Nitrosomonas* strain isolated from activated sludge. J Gen Microbiol 52:1–14

MacMillan F, Kannt A, Behr J, Prisner T, Michel H (1999) Direct evidence for a tyrosine radical in the reaction of cytochrome *c* oxidase with hydrogen peroxide. Biochemistry 38:9179–9184

Martinho M, Choi DW, DiSpirito AA, Antholine WE, Semrau JD, Münck E (2007) Mössbauer Studies of the membrane-associated methane monooxygenase from *Methylococcus capsulatus* Bath: evidence for a diiron center. J Am Chem Soc 129:15783–15785

McTavish H, Fuchs JA, Hooper AB (1993) Sequence of the gene coding for ammonia monooxygenase in *Nitrosomonas europaea*. J Bacteriol 175:2436–2444

Nelson MJ (1987) The nitric oxide complex of ferrous soybean lipoxygenase-1. J Biol Chem 262:12137–12142

Nguyen H-HT, Schiemke AK, Jacobs SJ, Hales BJ, Lidstrom ME, Chan SI (1994) The nature of the copper ions in the membranes containing the particulate methane monooxygenase from *Methylococcus capsulatus* (Bath). J Biol Chem 269:14995–15005

Nguyen H-HT, Nakagawa KH, Hedman B, Elliott SJ, Lidstrom ME, Hodgeson KOl, Chan SI (1996) X-ray absorption and EPR studies on the copper ions associated with the

particulate methane monooxygenase from *Methylococcus capsulatus* (Bath). J Am Chem Soc 118:12766–12776

Nguyen H-HT, Elliott SJ, Yip JH-K, Chan SI (1998) The particulate methane monoooxygenase from *Methylococcus capsulatus* (Bath) is a novel copper-containing three-subunit enzyme. J Biol Chem 273:7957–7966

Prior SD, Dalton H (1985) Acetylene as a suicide substrate and active site probe for methane monooxygenase from *Methylococcus capsulatus* (Bath). FEMS Microbiol Lett 29:105–109

Prosser JI (1989) Autotrophic nitrification in bacteria. Adv Microb Physiol 30:125–177

Que L (1983) Metalloproteins with phenolate coordination. Choordin Chem Rev 50:73–108

Que L, Jo RYN (1996) Dioxygen activation by enzymes with mononuclear non-heme iron active sites. Chem Rev 96:2607–2624

Sanders JKM, Bampos N, Clyde-Watson Z, Darling SL, Hawley JC, Kim H-J, Mak CC, Webb SJ (1999) Axial coordination chemistry of metalloporphyrins. In: Kadish KM, Smith KM, Gullard R (eds) The porphyrin handbook, vol 3. Academic Press, New York, pp 3–49

Schmidt I, Bock E (1997) Anaerobic ammonia oxidation with nitrogen dioxide by *Nitrosomonas eutropha*. Arch Microbiol 167:106–111

Schmidt I, Bock E (1998) Anaerobic ammonia oxidation by cell-free extracts of *Nitrosomonas eutropha*. Antonie van Leeuwenhoek. 73:271–278

Schmidt I, Bock E, Jetten MSM (2001) Ammonia oxidation by *Nitrosomonas eutropha* with NO_2 as oxidant is not inhibited by acetylene. Microbiology 147:2247–2253

Takeguchi M, Okura I (2000) Role of iron and copper in particulate methane monooxygenase of *Methylosinus trichosporium* OB3b. Catal Surv 4:51–63

Tumanova LV, Tukhvatullin IA, Burbaev DS, Gvozdev RI, Andersson KK (2008) The binuclear iron site of membrane-bound methane hydroxylase from *Methylococcus capsulatus* (strain M). Rus J Bioorg Chem 34:194–203

Yeager CM, Bottomley PJ, Arp DJ, Hyman MR (1999) Inactivation of toluene 2-monooxygenase in *Burkholderia cepacia* G4 by alkynes. Appl Environ Microbiol 65:632–639

Zahn JA, DiSpirito AA (1996) Membrane-associated methane monooxygenase from *Methylococcus capsulatus* (Bath). J Bacteriol 178:1018–1029

Zahn JA, Arciero DM, Hooper AB, DiSpirito AA (1996) Evidence for an iron center in the ammonia monooxygenase from *Nitrosomonas europaea*. FEBS Lett 397:35–38